

A Novel method for Computing Power System Frequency

S. S. Damhare, R. K. Gajbhiye, S. A. Gandhi, C. J. Tonde, S. A. Soman, *Member, IEEE*, M. C. Chandorkar, *Member, IEEE*

Abstract—Phasor-based estimation techniques are used for measuring instantaneous power system frequency. These methods are characterised by a very good steady state response and dynamic characteristics. The following paper proposes a novel phasor-based technique for frequency and rate of change of frequency estimation by estimating the amplitudes of both the voltage signal and its moving averaged signal. The proposed method is characterised by fixed speed, good accuracy and robustness. A well documented experimental results at the end prove the efficacy of this method.

Index Terms—Frequency estimation, rate of change in frequency, Discrete Fourier Transforms (DFT), fixed data window, moving average, magnitude estimation, adaptive window hugging, mean deviation.

I. INTRODUCTION

FREQUENCY is an important parameter in power systems. Accurate frequency estimation is imperative from the point of view of power systems protection. Various methods have been developed up till now for estimation of frequency and all have their distinct advantages. The modified zero-crossing technique [1], level crossing technique [2], least-square technique [3], Kalman filter technique [4], [5], and phasor based techniques [6]–[10] are fixed-frequency methods suitable for steady-state frequency measurement. Methods utilizing feedback loops such as [11]; Phase Locked Loop (PLL); phasor-based synchronized measurement [9] are methods which estimate dynamic changes in frequency. Among all of these methods, the phasor-based techniques appear to be more accurate. These methods follow a common way of estimating the positive-sequence phasor at off-nominal frequency, when the DFT is taken at nominal frequency. The phase angle change in the phasor is a function of deviation of frequency from nominal frequency. For a frequency modulated signal $x(t) = A \cos(\phi(t))$, where A represents the magnitude and ϕ represents the cumulative phase angles, instantaneous frequency is calculated as $f(t) = (1/2\pi)(d\phi/dt)$. In the following paper, we propose a novel method which takes the advantage of phasor-based technique to estimate amplitude of the original voltage signal and its moving average signal and hence the deviation in frequency. This method has advantage in terms of accuracy, speed and robustness over other methods mentioned in the paper. We first present a theoretical analysis

of the proposed method and then later support it with simulation results for a clean 3-phase signal and real signal from generator and a power system.

II. THE PROPOSED METHOD

A. Motivation

Let the nominal frequency be f_o and the actual system be at frequency f . The nominal time-period is given as

$$T_o = \frac{1}{f_o}$$

Let the sinusoidal voltage signal be given as

$$v(t) = V_m \sin(2\pi ft + \phi)$$

In order to calculate the moving average voltage, we perform an integration of the signal over the nominal time period T_o . This integral will be zero if the system is at nominal frequency. If the system is at off nominal frequency then we will show that the integral is another sinusoidal signal with a frequency f having an amplitude which is dependant on the system frequency. Therefore,

$$\begin{aligned} \frac{1}{T_o} \int_t^{t+T_o} V_m \sin(2\pi ft + \phi) dt \\ = V_m \text{sinc}(fT_o) \sin(2\pi ft + \varphi) \end{aligned}$$

Or

$$v_{avg}(t) = F_m \sin(2\pi ft + \varphi)$$

where v_{avg} is a moving cycle average, and F_m is the amplitude of the average voltage waveform given by,

$$F_m = V_m \text{sinc}(fT_o)$$

and φ is given as

$$\varphi = \phi + \pi fT_o$$

Thus the system frequency can be evaluated by estimating F_m and V_m and solving the equation

$$\frac{F_m}{V_m} = \text{sinc}(fT_o) \quad (1)$$

The frequency response of (1) is shown in Fig.1 taking nominal frequency value to be 50Hz.

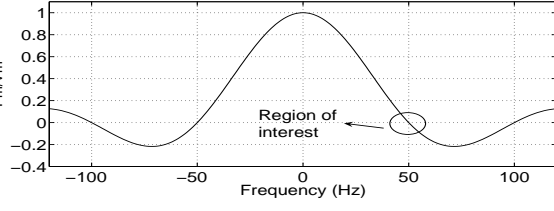


Fig. 1. Frequency response of 1

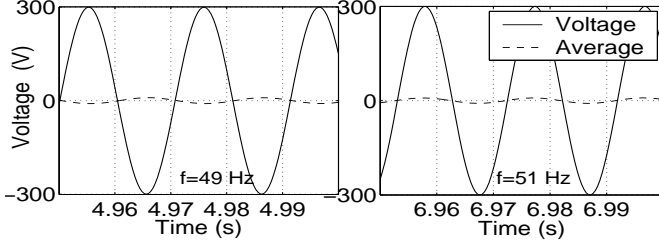


Fig. 2. Plot of Voltage and average voltage signal for 49 Hz and 51 Hz

It is to be noted that although V_m is positive through out, F_m is positive if $f < f_o$ and negative if $f > f_o$. Hence it can be concluded that in case of negative frequency deviation the voltage and the average voltage waveform are almost out of phase by π , and in the case of positive deviation they are almost entirely in phase, as shown in Fig.2. Therefore the computation of F_m involves computation of both the magnitude and sign of F_m . The value of $|V_m|$ and $|F_m|$ can be computed using Discrete Fourier Transform as follows.

1) *Estimation of V_m* : Let the available signal be sampled at a frequency f_s where

$$\frac{f_s}{f_o} = N \quad (2)$$

where N is the number of samples per cycle at nominal frequency, N being an integer. Let the voltage samples be given as V_k where $k = [1, 2, \dots]$. Now applying DFT on these samples we get

$$V_c^w(m) = \frac{2}{N} \sum_{k=w}^{N+w-1} v_k \cos\left(\frac{2\pi}{N} km\right)$$

$$V_s^w(m) = \frac{2}{N} \sum_{k=w}^{N+w-1} v_k \sin\left(\frac{2\pi}{N} km\right)$$

where w is the window number. Our convention is that we associate the window number with the first sample in that window. From this we get a recursive update as

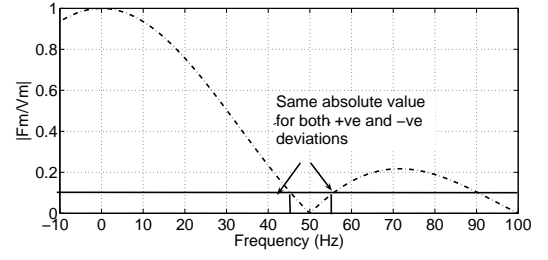
$$V_c^{w+1}(m) = V_c^w(m) + \frac{2}{N}(v_{w+N} - v_w) \cos\left(\frac{2\pi}{N} wm\right) \quad (3)$$

and similarly for sine component we have

$$V_s^{w+1}(m) = V_s^w(m) + \frac{2}{N}(v_{w+N} - v_w) \sin\left(\frac{2\pi}{N} wm\right) \quad (4)$$

from which we estimate V_m as follows,

$$V_m^w = \sqrt{V_c^{w2} + V_s^{w2}} \quad (5)$$

Fig. 3. Frequency response of $|F_m/V_m|$

2) *Calculation of F_m* : From the obtained samples of $v(t)$ we numerically integrate the signal using the trapezoidal rule of integration to get a moving average voltage signal. A recursive update for the integration is as follows,

$$v_{avg,k} = v_{avg,k-1} + \frac{1}{N} \left[\frac{v_k + v_{k-1}}{2} - \frac{v_{k-N} + v_{k-N-1}}{2} \right] \quad (6)$$

Now applying DFT on the samples generated from (6) we get the magnitude of F_m i.e. $|F_m|$. But for one value of $|F_m|$ we get two possible values of Δf as shown in Fig.3. Therefore we need to consider the proper sign of F_m before actually calculating frequency. In other words, we need to determine whether the voltage signal and its moving average signal are in-phase or out-of-phase. This can be done by first passing both the signals through a modified **Schmitt trigger** to eliminate false triggering at zero crossings and then a comparator as implemented below.

Let the digital output of the voltage signal from the Schmitt trigger be V_{sch} and that of the moving average voltage signal be $Av_{g_{sch}}$. Then F_m can be computed as follows:

$$F_m = -V_{sch} Av_{g_{sch}} |F_m| \quad (7)$$

When $f < f_o$, then $v(t)$ and $v_{avg}(t)$ signals will be out-of-phase, so that $V_{sch} Av_{g_{sch}} = -1$. Thus, F_m would be given as

$$F_m = |F_m|$$

and when $f > f_o$, then $v(t)$ and $v_{avg}(t)$ signals will be in phase, so that $V_{sch} Av_{g_{sch}} = 1$. Thus, F_m would be given as,

$$F_m = -|F_m|$$

Now taking the ratio of F_m and V_m we get,

$$\frac{F_m}{V_m} = \text{sinc}(fT_o) \quad (8)$$

from which frequency can be estimated.

3) *Estimating Frequency*: Let z be defined as follows,

$$z = \frac{F_m}{V_m}$$

$$z = \text{sinc}(fT_o) = \frac{\sin(\pi fT_o)}{\pi fT_o}$$

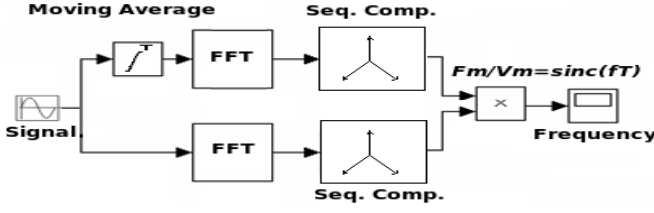


Fig. 4. Block model diagram

Replacing f by $f_0 + \Delta f$ we have

$$z = \frac{\sin(\pi(f_0 + \Delta f)T_o)}{\pi(f_0 + \Delta f)T_o}$$

Now since $f_0 T_o = 1$ therefore we can further simplify the expression as

$$z = -\frac{\sin(\pi \Delta f T_o)}{\pi + \pi \Delta f T_o}$$

Now since Δf is small we can approximate $\sin(\pi \Delta f T_o)$ as $\pi \Delta f T_o$. Hence, it can be further simplified as

$$z = -\frac{\pi \Delta f T_o}{\pi + \pi \Delta f T_o}$$

Therefore we obtain the value of Δf as

$$\Delta f = -\frac{z}{1+z} f_0 = -\frac{F_m}{V_m + F_m} f_0 \quad (9)$$

and hence the system frequency is given by

$$f = f_0 + \Delta f \quad (10)$$

B. Model Algorithm

The above idea can be summarized in as follows:

- 1) Obtain voltage (or current) samples from the system, The sampling frequency should be as given in (2).
- 2) The sampled data should be fed into the DFT generator to calculate V_m as mentioned in (3), (4), (5).
- 3) The voltage samples is simultaneously fed to the integrator which then performs the averaging as mentioned in (6).
- 4) The average voltage samples are then fed to the DFT which estimates $|F_m|$. F_m is then calculated with proper sign using (7).
- 5) The computed F_m and V_m is then used to calculate frequency as per (9) and (10).

C. Estimation of rate-of-change of frequency

Let the initial system frequency be $f = f_0 + \Delta f$. Suppose at $t = \tau$, frequency starts changing with rate r and continues till $t = \delta$, with $\delta > \tau$. If $U(t)$ is a unit function, $f(t)$ can be given by,

$$f(t) = (f_0 + \Delta f) + r(t - \tau)(U(t - \tau) - U(t - \delta)) + r(\delta - \tau)U(t - \delta)$$

Now for the time period $\tau < t < \delta$, the phase angle $\theta(t)$ given by ,

$$\begin{aligned} \theta(t) &= 2\pi\Psi(t) \\ \Psi(t) &= \int_0^t f(t)dt \\ &= (f_0 + \Delta f)t + \frac{r}{2}(t - \tau)^2 \end{aligned}$$

Let complex voltage signal will be represented as,

$$\begin{aligned} \bar{V}(t) &= V_m e^{j\theta(t)} = [V_m, \Psi(t)] \\ &= [V_m, (f_0 + \Delta f)t + \frac{r}{2}(t - \tau)^2] \end{aligned}$$

Thus

$$\bar{V}(t - \Delta t) = [V_m, (f_0 + \Delta f)(t - \Delta t) + \frac{r}{2}(t - \Delta t - \tau)^2]$$

where, Δt is the time interval.

Defining,

$$\begin{aligned} Z(t) &= \bar{V}(t - \Delta t) \bar{V}^*(t) \\ Z(t) &= [V_m^2, -(f_0 + \Delta f)\Delta t + \frac{r}{2}(\Delta t - 2(t - \tau))\Delta t] \\ &= [V_m^2, (-r\Delta t)t - (f_0 + \Delta f)\Delta t \\ &\quad + r(\Delta t)\tau + \frac{r}{2}(\Delta t)^2] \end{aligned}$$

Hence, the obtained signal $Z(t)$ is oscillating with frequency $r\Delta t$ and has magnitude V_m^2 . Since r is expected to be very small, frequency of $Z(t)$ is very close to 0. Hence, we frequency shift this signal by f_0 , by simply multiplying it by $< 1, f_0 t >$. Thus,

$$\begin{aligned} Z_{shift}(t) &= [V_m^2, (f_0 - r\Delta t)t - (f_0 + \Delta f)\Delta t \\ &\quad + r(\Delta t)\tau + \frac{r}{2}(\Delta t)^2] \end{aligned}$$

We can use above mentioned frequency estimation technique to estimate $r\Delta t$ and hence, r .

D. Oscillations in DFT response

When considering a single phase signal it can be shown that the DFT response i.e. $|V_m^w|$ and $|F_m^w|$ will be oscillatory. These oscillations are because of the presence of a higher frequency components. This is evident from the analysis presented in A. It is also shown how these oscillations can be removed by using all the three phases for estimating magnitudes $|V_m^w|$ and $|F_m^w|$.

E. Computations for unbalanced systems

For unbalanced system we can directly use SC DFT as mentioned in [12]. For unbalanced system, a recursive update can be used which is given in D. Or other wise we can use DFT SC, i.e. we shall first apply DFT on the voltage samples and construct the phasors. Then we extract the positive sequence components from these phasors.

$$\begin{aligned} V_A &= V_{As} + jV_{Ac} \\ V_B &= V_{Bs} + jV_{Bc} \\ V_C &= V_{Cs} + jV_{Cc} \end{aligned}$$

Then we can extract the positive sequence components as follows,

$$\begin{aligned} V_A^+ &= \frac{1}{3}(V_{As} + aV_{Bs} + a^2V_{Cs} + j(V_{Ac} + aV_{Bc} + a^2V_{Cc})) \\ V_B^+ &= \frac{1}{3}(V_{Bs} + aV_{Cs} + a^2V_{As} + j(V_{Bc} + aV_{Cc} + a^2V_{Ac})) \\ V_C^+ &= \frac{1}{3}(V_{Cs} + aV_{As} + a^2V_{Bs} + j(V_{Cc} + aV_{Ac} + a^2V_{Bc})) \end{aligned}$$

F. Computations for single phase systems

In single phase systems, as explained before, there will be oscillations which can only be avoided by using three phase information. Therefore for single phase analysis the other three phases should be constructed by giving the phasor at hand a ± 120 degree shift. In discrete domain, however to get a $+\frac{2\pi}{3}$ shift the $(k - \frac{N}{3})^{th}$ sample should be considered and for a $-\frac{2\pi}{3}$ shift the $(k - \frac{2N}{3})^{th}$ sample. Hence, considering the voltage samples available at hand as the A phase voltage, the other phases can be constructed as follows.

$$\begin{aligned} v_B^k &= v_A^{k - \frac{N}{3}} \\ v_C^k &= v_A^{k - \frac{2N}{3}} \end{aligned}$$

Now since the system is at offnominal frequency therefore the $(k - \frac{N}{3})^{th}$ would not give the required $\frac{2\pi}{3}$ phase shift. So evidently the three phase system obtained would be unbalanced in phase. Therefore we need to take the SCDFT or the DFTSC and then pass the balanced phases to the blackbox containing the algorithm for frequency estimation.

G. Time response

For full cycle DFT the time required to latch on to a value is one cycle. So, in estimating V_m we have one cycle delay in measurement. Again while we integrate to calculate the moving average we have one cycle delay. Therefore when we calculate F_m we have another one cycle delay. So, measurement of F_m will take in total two cycles to latch on. Therefore the estimated value of frequency will also take two cycles to latch on.

H. Frequency Response

The frequency response of the system is a **sinc** curve, in the form of $\text{sinc}(fT_o)$ which is depicted in the Fig.1. It is evident that the higher frequency components are attenuated. This is the inherent advantage of the method. However, from the frequency response curve it is clear that the performance of the method will be better in the presence of high frequency components if the lobes in the frequency response curve are attenuated. This can be done by:

- Increasing the time of integration.
- Sensitivity Enhancement.
- Integrating twice in which case we get the frequency response as $[\text{sinc}(fT_o)]^2$.

Let us explore each possibilities one by one.

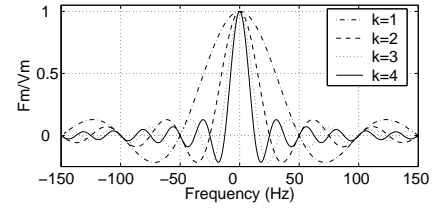


Fig. 5. Frequency response with different integration periods

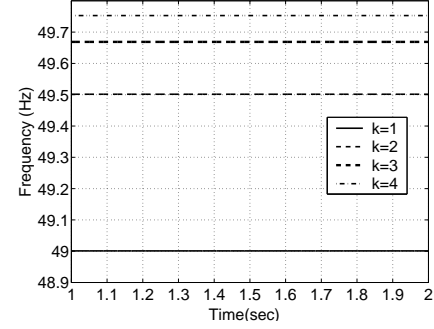


Fig. 6. Over estimation caused due to different integration periods

1) *Increasing the time of Integration:* By increasing the time of integration we indeed found out that the higher frequency lobes in the frequency response are getting attenuated and we get the following curve,

Fig.5 has four plots. If we consider a variable k as the number of cycles over which the averaging is done, then the blue plot is for $k = 1$, red for $k = 2$, green for $k = 3$, and black for $k = 4$. Therefore we see that at higher values of k the lobes at higher frequencies get more attenuated and the result improves. In the time domain, doing the integration over k^{th} complete cycle will give

$$\begin{aligned} &\frac{1}{kT_o} \int_t^{t+kT_o} V_m \sin(2\pi ft + \phi) dt \\ &= V_m \text{sinc}(kfT_o) \sin(2\pi ft + \phi) \end{aligned}$$

Hence increasing the time of integration also changes the frequency response. The new response now is $\text{sinc}(kfT_o)$. However, it has been seen that with increasing the time of integration i.e. with increasing k the tendency to overestimate the frequency value also increases. This is illustrated in Fig.6.

2) *Sensitivity Enhancement:* **Sensitivity** of the method is directly dependant on the slope of the frequency response curve at the nominal frequency. So the motivation would be to increase the slope of the frequency response curve at around the nominal frequency. But although increasing the period of integration from T_o to kT_o improves the **Harmonics and higher frequency components rejection** the noise filtering property of the system does not change as the slope of the new frequency response curve obtained i.e. $\text{sinc}(kfT_o)$ is same at the nominal frequency.

$$\left| \frac{d}{df} \text{sinc}(kfT_o) \right| = f_o \quad \forall k \quad (11)$$

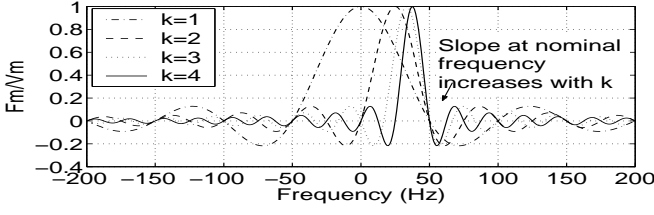


Fig. 7. Frequency response of shifted sinc curves for different integration periods

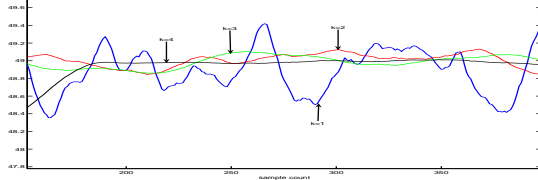


Fig. 8. Plot for estimated frequency in presence of noise

Therefore it is evident that simply increasing the window size will not improve the estimation. Therefore, what we need is to increase the window size and simultaneously increase the slope of the curve at 50 Hz. Looking at the frequency response for different values of k as in Fig.5 we see that although the slope at $f = f_o$ is same the curves do successively attain higher slopes with increasing k . We can therefore use the high slopes at around f_o by shifting the curve by required amount. Intuitively this is found possible if we can synthesize a function such as

$$v(t) = V_m \sin(2\pi(f - (1 - \frac{1}{k})f_o)t + \phi) \quad (12)$$

where k is the number of cycles over which the averaging is done. On integrating over kT_o

$$V_{avg} = \frac{1}{kT_o} \int_t^{t+kT_o} V_m \sin(2\pi(f - (1 - \frac{1}{k})f_o)t + \phi) dt$$

$$V_{avg} = V_m \text{sinc}(k(f - (1 - \frac{1}{k})f_o)T_o) \sin(2\pi ft + \phi)$$

By taking the derivative at $f = f_o$ it is seen that

$$\frac{d}{df} \text{sinc}(k(f - (1 - \frac{1}{k})f_o)T_o) = -\frac{k}{f_o} \quad (13)$$

Therefore as we increase k the slope indeed increases as shown in Fig.7 Thus with successively increasing k the slope at nominal frequency increases and hence increasing the noise rejection property. And also from actual computer generated samples, the result was confirmed that in presence of noise the output is much more stable, as shown in Fig.8

Synthesizing the composite signal from the original one is explained below. In time domain, the signal that is required is,

$$v(t) = V_m \sin(2\pi(f - (1 - \frac{1}{k})f_o)t + \phi) \quad (14)$$

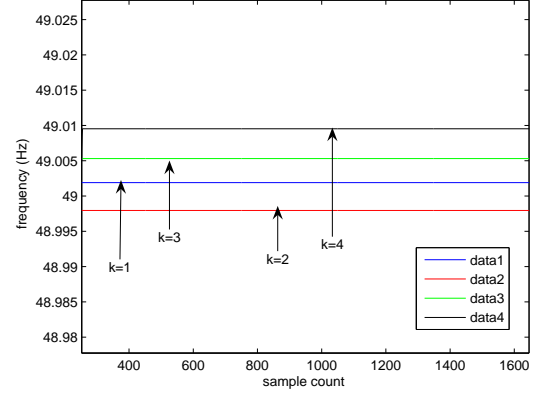


Fig. 9. Plot for estimated frequency for (12)

Expanding,

$$v(t) = V_m \left[\sin(2\pi ft + \phi) \cos(2\pi(1 - \frac{1}{k})f_o t) \right] - \left[\cos(2\pi ft + \phi) \sin(2\pi(1 - \frac{1}{k})f_o t) \right]$$

The expression $\sin(2\pi ft + \phi)$ is directly obtained from the signal itself. We can simply multiply it with the expression $\cos(2\pi(1 - \frac{1}{k})f_o t)$. However to generate the $\cos(2\pi ft + \phi)$ expression, we can take the help of the other two phases, i.e. if

$$\begin{aligned} v_a(t) &= V_m \sin(2\pi ft + \phi) \\ v_b(t) &= V_m \sin(2\pi ft + \phi - \frac{2\pi}{3}) \\ v_c(t) &= V_m \sin(2\pi ft + \phi + \frac{2\pi}{3}) \end{aligned}$$

Therefore, in this case,

$$V_m \cos(2\pi ft + \phi) = \frac{v_c(t) - v_b(t)}{\sqrt{3}} \quad (15)$$

Similarly repeating the above process it can be done for other phases as well. Once the quadrature component for each phases are obtained the desired signal can be easily generated. However, as mentioned before, the algorithm has a tendency to overestimate for increasing values of k . This is illustrated in Fig.9. ¹

3) *Integrating two times:* In this case, the signal is averaged out two times. The frequency response becomes $[\text{sinc}(fT_o)]^2$ and the lobes at higher frequencies are highly attenuated, as illustrated in Fig.10 However, it is seen that the slope of the frequency response is zero at 50 Hz, hence deteriorating the noise filtering property. Hence to remedy this the curve can be shifted (refer Fig.10). But the problem here is that with shifting, harmonic rejection becomes poor. Therefore in comparison with the previous method (i.e. increasing integration time) this method is not so efficient.

¹If the shifted signal is used then with higher values of k , N should also be increased, or we can define N as $N = kN$.

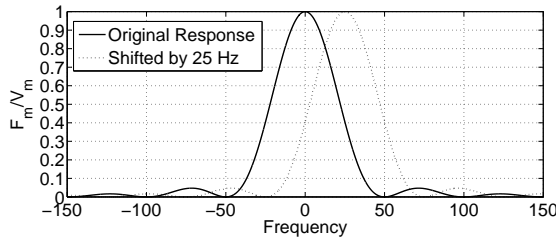


Fig. 10. Frequency response after averaging out two times

I. Effect of introducing anti aliasing filters in the system

Anti aliasing filters can also be integrated into the system. If an anti aliasing filter of cutoff frequency half of the sampling frequency be introduced in the system, then the higher frequency components would be reduced and in the algorithm the k value could be kept to unity. This will further reduce errors in estimation as higher k values will lead to overestimation of frequency.

J. Time Response for the shifted signal

Time response of the shifted signal would be different from the original one. If the integration period is over k complete cycles then the delay in measurement would be $2k$. In case we do not do the shifting, then an integration over k cycles will give $k + 1$ cycle delay in measurement. Therefore it is seen that with increasing k accuracy increases in presence of noise but at the sacrifice of time. However this can be remedied by introducing a **adaptive window hugging and minimum variance tracking** technique as mentioned below.

1) *Adaptive Window Hugging and minimum variance tracking technique:* A recursive update for mean and variance of the estimated frequency values is developed as follows

$$\mu_{w+1} = \mu_w + \left[\frac{f_{w+1} - f_{w-N+1}}{N} \right]$$

$$\sigma_{w+1}^2 = \sigma_w^2 + \left[\frac{f_{w+1}^2 + f_{w-N+1}^2}{N} \right] - (\mu_{w+1}^2 - \mu_w^2)$$

From this we can keep a track of the standard deviation of the frequency values. Therefore, we concurrently run three or four processes for different values of k , and keep a track of the standard deviation of the frequency values. The sample having minimum standard deviation would be picked up and given as the output.

K. The Modified Algorithm

Incorporating the above techniques we can devise an algorithm as follows.

- First the voltage samples are obtained. The sample voltages are processed as mentioned in (14),(15), for different k values.
- The processed signal samples (for different k values) are sent in different black boxes for the corresponding k values.
- The output of the blackboxes are fed to a comparator which compares the standard deviation of the estimated

TABLE I
FREQUENCY MEASUREMENT RESULTS

Sr. No.	Frequency	Measured	% Error
1	47.0	47.0033	+0.0070
2	48.0	48.0023	+0.0048
3	49.0	49.0012	+0.0024
4	49.5	49.5006	+0.0012
5	50.0	50.0000	0.0000
6	50.5	50.4993	-0.0014
7	51.0	50.9986	-0.0028
8	52.0	51.9970	-0.0060
9	53.0	52.9952	-0.0091

frequency values. The sample corresponding to the minimum standard deviation would be picked up and given as output.

III. SIMULATION VERIFICATION

The simulation of the above proposed method is carried out in MATLAB with $N=50$ samples/cycle and nominal frequency 50Hz. The proposed algorithm is tested for constant and linearly and non-linearly changing frequency input. The following are the results from the tests.

1) *Constant Frequency:* Three phase balanced sinusoid's were generated using the following Eqns.

$$\begin{aligned} V_a(t) &= V_m \cos(2\pi ft) \\ V_b(t) &= V_m \cos(2\pi ft - 2\pi/3) \\ V_c(t) &= V_m \cos(2\pi ft + 2\pi/3) \end{aligned} \quad (16)$$

The proposed algorithm was applied to these signals with $V_m = 300$ V and Schmitt trigger threshold value set at $V_{th} = 220$ V. The measured response was captured for different frequencies and the results were obtained as shown in Table I. We can clearly see that the estimated values are approximately equal to the input values within %error of 0.01% in the frequency range 47-53 Hz. This accuracy limit is forced due to the lookup table implementation of sinc function to find arcsinc. An increase in the resolution of sinc lookup table would increase the accuracy while sacrificing on computation time.

2) *Linearly Increasing Frequency:* The generated three phase signals are as in (16), where

$$f = \begin{cases} 47 & 0 \leq t < 4 \\ 47 + r * (t - 4) & 4 \leq t < 8 \\ 53 & 8 \leq t < 12 \end{cases} \quad (17)$$

where,

$r = 1.5$ is the rate of change in frequency in Hz/sec. The results are as shown in Fig.11

The proposed method and rate-of-change of frequency were applied to case of linearly increasing frequency. In this case the measured frequency faithfully follows the input frequency. The dynamic response of the system in time $4 \leq t < 8$ seconds is approximately linear and takes latching time of 2 cycles ($k = 1$). To determine whether the deviation of frequency is positive or negative we use Schmitt trigger on the input signal (V_a) and its averaged signal. In a schmitt trigger the sign determination takes place only when the following condition is met.

$$|V_a| \geq V_{th} \quad (18)$$

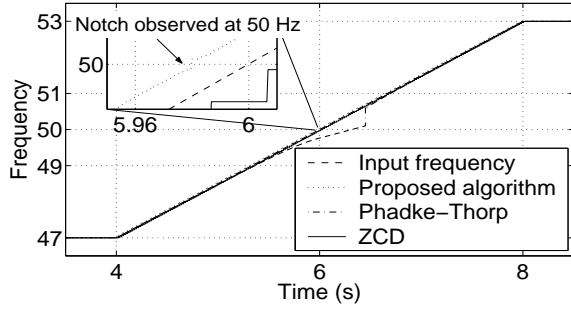


Fig. 11. Linearly increasing frequency

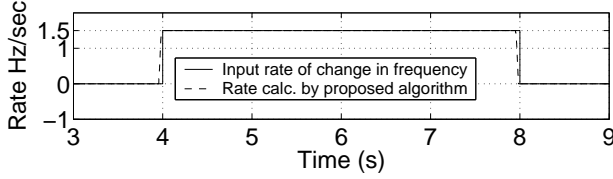


Fig. 12. Rate-of-change estimation for (17)

In case of linearly increasing frequency that crosses 50 Hz, the magnitude of average signal reduces to zero. The sign determination doesn't take place if $|V_a| < V_{th}$ at that instant and get delayed by a few samples till condition in (18) is met again. This causes a small notch to occur at near about 50 Hz (Fig.11). The magnitude of this notch is around 0.05 Hz. Reducing the threshold value V_{th} would certainly reduce the notch size but would cause false triggering in noisy signals. A better technique for deviation sign determination would certainly be a solution to this. The r estimation algorithm worked as expected for clean signal of increasing frequency. The rate of change of frequency was estimated accurately with delay of 3 cycles: One cycle for the preprocessing of the signal using equations in Section [II-C] and 2 cycles for frequency estimation algorithm. The Fig.12 illustrates this for $r = 1.5$.

3) *Non-Linearly Increasing Frequency*: The three phase signals generated are similar to those given in the previous subsection [III-2] except for the fact that the rate of change in frequency r is not constant but varied with time given as follows,

$$f = \begin{cases} 54 & 0 \leq t < 4 \\ 54 + r * (t - 4) & 4 \leq t < 8 \\ 46 & 8 \leq t < 12 \end{cases} \quad (19)$$

where,

$$r = \begin{cases} 0 & 0 \leq t < 4 \\ -2.5 + 0.1 * (t - 4) * (t - 8) & 4 \leq t < 8 \\ 0 & 8 \leq t < 12 \end{cases} \quad (20)$$

The results are illustrated in the Fig.13. Here, we find that the frequency estimated by our proposed algorithm faithfully follows the non-linear input. The instantaneous rate of change in frequency is also illustrated in Fig.14. The rate r has very high value at $t = 8$ seconds due to the fact that there is a step change in the frequency at $t = 8$ as seen in the Fig.13.

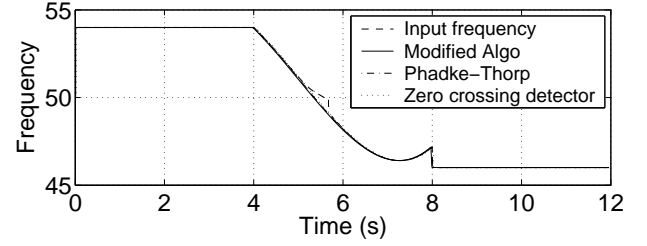


Fig. 13. Frequency plot for non-linear frequency input

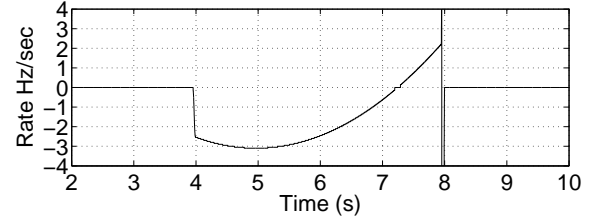


Fig. 14. Rate-of-change estimation for non-linear frequency input

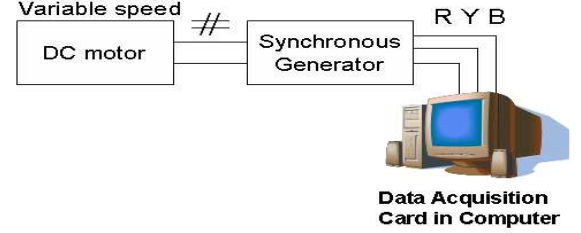


Fig. 15. Experiment setup

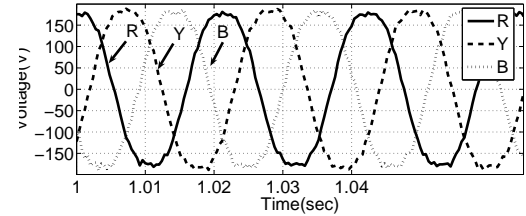


Fig. 16. Three phase voltages

IV. LABORATORY EXPERIMENT

A laboratory experiment was performed to carry out a performance study of the proposed method using real voltage samples. Fig.15 below outlines the experimental setup for collection of voltage data samples. A synchronous generator at no-load coupled with a DC motor was used to generate balanced three-phase voltage signals with constant and varying frequency. Three-phase voltages were signal conditioned and sampled using a data-acquisition card with constant sampling rate of $N=50$ samples per cycle and were recorded on the computer. The ADC resolution used was 10-bit. Simulations were carried out in MATLAB with collected data and results obtained were then compared to other methods: Phadke-Thorp method [12], Phase Locked Loop, Zero-crossing detector.

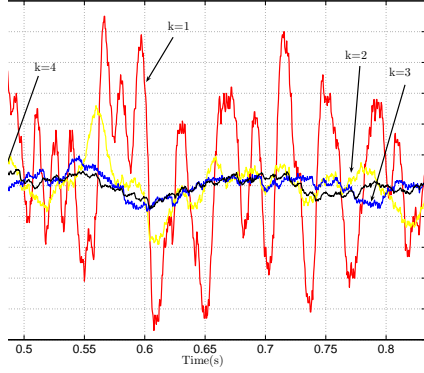


Fig. 17. Response for different k values

A. Constant Frequency

Steady state response of algorithm to generator generated signals (Fig.16) is shown in Fig.18(a). Three other methods were used for a accuracy comparison of the measured frequency. Fig.18(b) is the phasor method of Phadke-Thorp [12] which used DFT as nominal frequency f_0 and then measures the time taken for phasor to rotate by θ radians ($\theta=0.5$ rad in this case). This method used a sum the previous samples phase-change and counts the time taken to complete $\theta=0.5$ rad. Hence the response is quite steady and smoothed out. Fig.18(c) is a response to a tuned Phase Locked Loop, the response is as expected steady by sight oscillatory. And finally as zero-crossing detector implementation is shown in Fig.18(d). All these and results for several other frequencies have been summarized in table II. Generator speed measured by means of a tachometer and calculated frequency by using Eqn. 21.

$$f = NP/120 \quad (21)$$

where N =generator speed(rpm), P = number of poles, f = frequency(Hz).

Increasing the window size over k cycles where $k = 1, 2, 3, 4$. and using sensitivity enhancement technique of section II-H2, the averaging effect is clearly seen in Fig.17. The oscillations in frequency have reduced but at the expense of added delay ($2k$ cycles.). Above $k = 4$ cycles the technique overestimates the frequency value and hence k is restricted at $k = 4$ cycles.

B. Linearly Varying Frequency

For simulating linearly varying frequency, the resistance in series with the field winding of DC motor was varied. The variation was done manually for approximately linear output. A linear change in the speed of the synchronous generator is assumed on account of its rotor inertia. It is evident from the Fig.19 that the frequency estimated by Phadke-Thorp method [12] is not accurate around 50Hz. The frequency estimated by PLL is used as the reference in this range. The measured frequency by the proposed algorithm follows the input quite accurately estimated by the algorithm. The rate-of-change of frequency measured for the Fig.19. For different values of k ($k = 1, 2, 3, 4$.) the measured value of rate of change of

TABLE II
FREQUENCY MEASUREMENT RESULTS FOR GENERATOR AVERAGED OVER ONE SEC.

Gen. RPM	Calculated frequency	Proposed method	Phadke-Thorp	PLL detector	Zero-cross.
1312	43.7333	43.7579	43.7500	43.7525	43.7520
1337	44.5667	44.5941	44.5584	44.5885	44.5893
1346	44.8667	44.8998	44.8637	44.8951	44.8987
1369	45.6333	45.6677	45.6363	45.6623	45.6619
1386	46.2000	46.1463	46.1376	46.1429	46.1406
1398	46.6000	46.7203	46.7598	46.7173	46.7181
1423	47.4333	47.4143	47.4044	47.4124	47.4121
1450	48.3333	48.1893	48.1727	48.1869	48.1896
1467	48.9000	48.9245	48.9201	48.9233	48.9238
1479	49.3000	49.3213	49.3383	49.3214	49.3231
1490	49.6667	49.6921	49.7074	49.6931	49.6911
1501	50.0333	50.1754	50.2032	50.1875	50.1887
1520	50.6667	50.6036	50.6323	50.6038	50.6046
1539	51.3000	51.2378	51.2096	51.2386	51.2398
1560	52.0000	51.9918	51.9967	51.9950	51.9937
1590	53.0000	53.0364	53.0351	53.0408	53.0415
1602	53.4000	53.4046	53.4107	53.4098	53.4146
1622	54.0667	54.0870	54.0679	54.0934	54.0965

frequency was found to be close to accurate with higher values of k . This is shown in Fig.21. The algorithm gives fair amount of qualitative information regarding the change of frequency.

C. System Frequency

As a verification, samples collected from three-phase system supply were fed to the algorithm. The results obtained are as shown in the Fig.22. The frequency measured is compared with phasor method of Phadke-Thorp [12]. The measured frequency is quite close to actual frequency measured by phasor method of Phadke-Thorp.

V. CONCLUSIONS

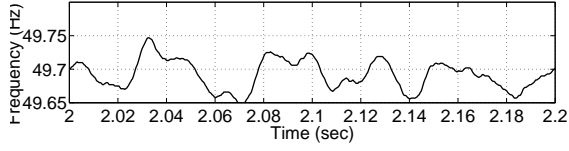
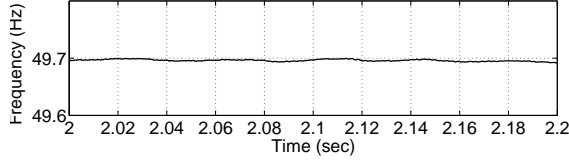
This paper has proposed a new method of computing system frequency that considers dynamic performance of the reported frequency. The following results were obtained:

- 1) the proposed method is found to be accurate with error% within 0.01% for frequencies in the range of 47-53 Hz and its accuracy fairly depends upon the accuracy of the lookup table of sinc used.
- 2) The time for estimating frequency is independent of the value of frequency. Once the required accuracy is set, the data window size i.e. value of k can be fixed.
- 3) by varying the data window size from one cycle ($k = 1$) till four cycles ($k = 4$) the algorithm gave better results but at the expense of a delay of $2k$ cycles.
- 4) for estimating the rate-of-change of frequency the algorithm showed encouraging results for clean signals and noisy signals when $k = 3$ or $k = 4$ cycles.

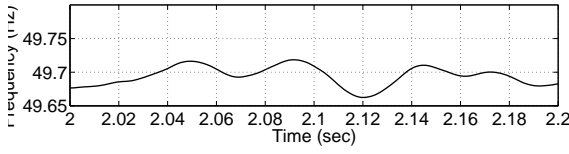
APPENDIX A OSCILLATION INHERENT IN DFT

Let there be a voltage signal defined as

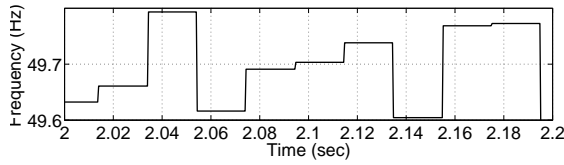
$$v(t) = V_m \cos(2\pi ft + \phi)$$

(a) Proposed method with $k = 1$ 

(b) Phadke-Thorp method



(c) Phase Locked Loop



(d) Zero-crossing detector

Fig. 18. Plot of frequency estimated by various frequency detection algorithms using generator data corresponding to 48.9 Hz

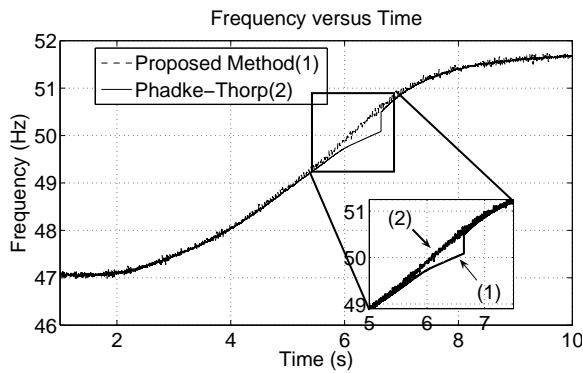


Fig. 19. Linear varying frequency of generator

Therefore we write it as

$$v(t) = V_m \frac{e^{j(\omega t + \phi)} + e^{-j(\omega t + \phi)}}{2}$$

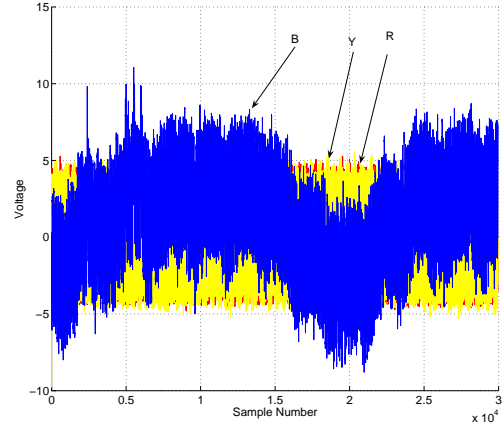


Fig. 20. Averaged signal of the generator

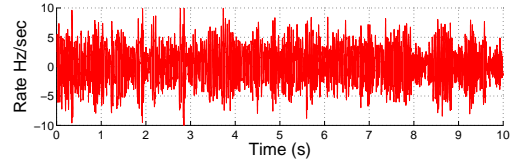
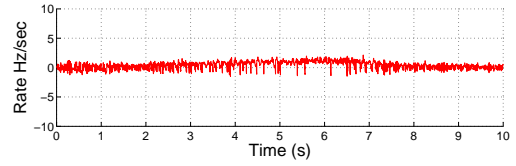
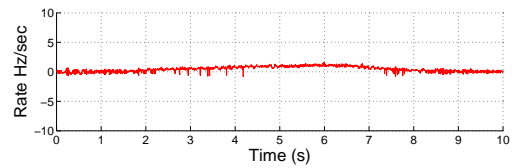
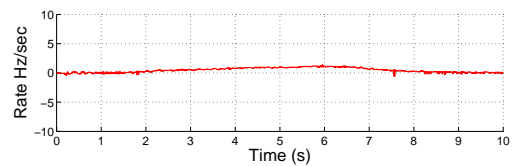
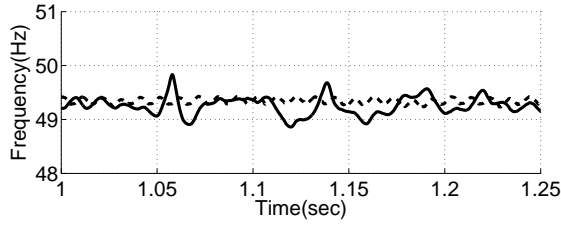
(a) $k = 1$ (b) $k = 2$ (c) $k = 3$ (d) $k = 4$

Fig. 21. Rate of change of frequency estimation for generator signals

Now if we apply DFT on the signal taking the first sample of the l^{th} window as the starting point. Let us define k as

$$k = \frac{f}{f_o}$$

Fig. 22. Power system frequency ($k = 1$)

and N as the number of samples per cycle assuming system to be at nominal frequency. Now applying full cycle DFT on the signal, in discrete domain, we have

$$V_1^w = V_m \frac{1}{N} \left[e^{j\phi} \sum_{n=w}^{N-w+l} e^{j \frac{2\pi(k-1)}{N} n} \right] + V_m \frac{1}{N} \left[e^{-j\phi} \sum_{n=w}^{N-w+l} e^{-j \frac{2\pi(k+1)}{N} n} \right] \quad (22)$$

The above expression simplifies as follows (for detailed analysis refer B).

$$V_1^w = V_m \frac{1}{N} e^{j(\phi + \frac{2\pi(k-1)(w - \frac{N}{2})}{N})} \left[\frac{\sin(\pi(k-1))}{\sin(\frac{\pi(k-1)}{N})} \right] \quad (23)$$

$$+ V_m \frac{1}{N} e^{-j(\phi + \frac{2\pi(k+1)(w - \frac{N}{2})}{N})} \left[\frac{\sin(\pi(k+1))}{\sin(\frac{\pi(k+1)}{N})} \right] \quad (24)$$

Now we define

$$A = \frac{1}{N} \frac{\sin(\pi(k-1))}{\sin(\frac{\pi(k-1)}{N})}$$

$$B = \frac{1}{N} \frac{\sin(\pi(k+1))}{\sin(\frac{\pi(k+1)}{N})}$$

$$\psi_1^w = \frac{2\pi(k-1)(w - \frac{N}{2})}{\frac{N}{2}}$$

$$\psi_2^w = \frac{2\pi(k+1)(w - \frac{N}{2})}{\frac{N}{2}}$$

Now the magnitude of the phasor is given as $V^w \cdot V^{w*}$ or

$$V_l^w \cdot V_l^{w*} = |V_1^w|^2 = V_m^2 [Ae^{j(\phi + \psi_1^w)} + Be^{-j(\phi + \psi_2^w)}] [Ae^{-j(\phi + \psi_1^w)} + Be^{j(\phi + \psi_2^w)}]$$

or

$$V_l^w \cdot V_l^{w*} = |V_1^w|^2 = V_m^2 [(A^2 + B^2) + 2AB \cos(\psi_1^w - \psi_2^w)]$$

Now in this magnitude expression we have a constant part i.e. $(A^2 + B^2)$ and a variable part which is dependant on the window number (i.e. $e^{j(2\phi + \psi_1^w + \psi_2^w)} + e^{-j(2\phi + \psi_1^w + \psi_2^w)}$). This part manifests as oscillation in the output. This anomaly is inherent in the DFT process. One way to eliminate these oscillations is to use three phase information.

$$|\tilde{V}| = \sqrt{\frac{|V_A^w|^2 + |V_B^w|^2 + |V_C^w|^2}{3}} \quad (25)$$

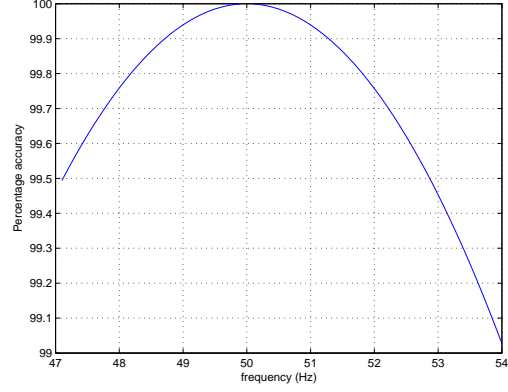


Fig. 23. Percentage Accuracy vs Frequency plot

It can be easily shown that

$$V_A^w V_A^{w*} = |V_A^w|^2 = V_m^2 [(A^2 + B^2) + 2AB \cos(\psi_1^w - \psi_2^w)]$$

$$V_B^w V_B^{w*} = |V_B^w|^2 = V_m^2 [(A^2 + B^2) + 2AB \cos(\psi_1^w - \psi_2^w)]$$

$$V_C^w V_C^{w*} = |V_C^w|^2 = V_m^2 [(A^2 + B^2) + 2AB \cos(\psi_1^w - \psi_2^w)]$$

where $a = e^{j\frac{2\pi}{3}}$. Now adding the above three equations we have

$$|\tilde{V}|^2 = V_m^2 [3(A^2 + B^2) + (1 + a + a^2)AB[e^{j(\psi_1^w + \psi_2^w)}] + V_m^2 [(1 + a + a^2)AB[e^{-j(\psi_1^w + \psi_2^w)}]]]$$

Therefore as $1 + a + a^2 = 0$ the oscillatory components vanish and we get a stable output. Therefore we see that the factor that comes as $A^2 + B^2$ manifests as error in the measurement. Plotting $\sqrt{A^2 + B^2}$ for different values of frequency (i.e. between 47 Hz to 53 Hz) we see that the values of the expression comes almost close to 1 as shown in Fig. (23). Hence we can approximate V_m as,

$$V_m^2 = \frac{\tilde{V}^2}{3} \quad (26)$$

The important point to note here is that the above analysis works only for balanced system. In case of an unbalanced system we should compute the balanced sequence components (positive sequence) using SCDF (Sequence Components Discrete Fourier Transform).

APPENDIX B SIMPLIFYING EQUATION

The expression obtained in (22) i.e.

$$V_1^w = V_m \frac{1}{N} \left[e^{+j\phi} \sum_{n=w}^{N-w+l} e^{j \frac{2\pi(k-1)}{N} n} \right] + V_m \frac{1}{N} \left[e^{-j\phi} \sum_{n=w}^{N-w+l} e^{-j \frac{2\pi(k+1)}{N} n} \right]$$

can be solved as follows. The first summation is infact a series summation of geometric progression which can be simplified as

$$S_1 = \frac{2}{N} e^{+j\phi} \sum_{n=w}^{N-w+l} q^n$$

where q is $e^{j2\pi \frac{k-1}{N} n}$. Therefore we get S_1 as

$$S_1 = \frac{1}{N} e^{+j\phi} q^w \left[\frac{1 - q^N}{1 - q} \right]$$

Similarly for the other summation S_2 we have

$$S_2 = \frac{1}{N} e^{-j\phi} p^w \left[\frac{1 - p^N}{1 - p} \right]$$

where p is $e^{-j2\pi \frac{k+1}{N} n}$. Therefore

$$V_1^w = V_m \frac{1}{N} e^{+j\phi} q^w \left[\frac{1 - q^N}{1 - q} \right] + V_m \frac{1}{N} e^{-j\phi} p^w \left[\frac{1 - p^N}{1 - p} \right]$$

Here V_1^w is a function of w i.e. the window number. Again we can write

$$V_1^w = V_m \frac{1}{N} e^{+j\phi} q^w \frac{q^{\frac{N}{2}}}{q^{\frac{1}{2}}} \left[\frac{q^{-\frac{N}{2}} - q^{\frac{N}{2}}}{q^{-\frac{1}{2}} - q^{\frac{1}{2}}} \right] + V_m \frac{1}{N} e^{-j\phi} p^w \frac{p^{\frac{N}{2}}}{p^{\frac{1}{2}}} \left[\frac{p^{-\frac{N}{2}} - p^{\frac{N}{2}}}{p^{-\frac{1}{2}} - p^{\frac{1}{2}}} \right]$$

Now substituting the values of p and q we have the expression simplified as mentioned in (23) i.e.

$$V_1^w = V_m \frac{1}{N} e^{+j(\phi + \frac{2\pi(k-1)(w-\frac{N}{2})}{N})} \left[\frac{\sin(\pi(k-1))}{\sin(\frac{\pi(k-1)}{N})} \right] + V_m \frac{1}{N} e^{-j(\phi + \frac{2\pi(k+1)(w-\frac{N}{2})}{N})} \left[\frac{\sin(\pi(k+1))}{\sin(\frac{\pi(k+1)}{N})} \right]$$

APPENDIX C

OTHER ALGORITHMS ON FREQUENCY MEASUREMENT

Amongst the existing algorithms for frequency estimation the Phadke Thorp's method is the most popular. The basic idea behind Phadke Thorpe's method of frequency estimation is that if we take a DFT on the positive sequence voltage at offnominal frequencies then the obtained phasor rotates in the complex plane with an angular velocity which directly proportional to the frequency deviation. Let the nominal frequency be ω_o . then we can write the phase voltages as,

$$V_a(t) = \frac{1}{2} [V e^{j\omega t} + V^* e^{-j\omega t}] \\ V_b(t) = \frac{1}{2} [V \alpha^2 e^{j\omega t} + V^* \alpha^{*2} e^{-j\omega t}] \\ V_c(t) = \frac{1}{2} [V \alpha e^{j\omega t} + V^* \alpha^* e^{-j\omega t}]$$

where V is the positive sequence voltage and α is $e^{j\frac{2\pi}{3}}$, and ω is the offnominal frequency different from ω_o . Now if we apply

DFT to calculate the positive sequence voltage corresponding to N samples per cycle, for the L^{th} window then we have

$$V^L = \frac{2}{k} \sum_{n=l}^{N-1+l} \frac{1}{3} [V_a(N\Delta t) + \alpha V_b(N\Delta t) + \alpha^2 V_c(N\Delta t)] e^{-jn\omega_o \Delta t}$$

Now substituting the values of V_a , V_b and V_c we get the following simplified form,

$$V^L = \frac{1}{N} \sum_{n=l}^{N-1+l} V e^{jn\Delta\omega \Delta t}$$

This sum can be computed as

$$V^L = V e^{jl\Delta\omega \Delta t} \left[\frac{\sin(\frac{N\Delta\omega \Delta t}{2})}{N \sin(\frac{N\Delta\omega \Delta t}{2})} e^{-j(N-1)\Delta\omega \frac{\Delta t}{2}} \right] \quad (27)$$

The bracketed term in (27) is the error in estimating the phasor. Therefore it is evident that the obtained phasor does have a rotation proportional to the frequency deviation.

Let the phase angle of the voltage phasor be ψ , then,

$$\psi_w = \psi_{w-1} + \Delta\omega \Delta t$$

or in other words

$$\frac{d\psi}{dt} = \frac{\psi_w - \psi_{w-1}}{\Delta t} = \Delta\omega$$

Therefore we see that if Δf is +1 then the phasor rotates counterclockwise in the plane at the rate of one revolution per second. If the Δf is -1 then the rotation is clockwise. Now if the system is exposed to noise then merely differentiating the slope will further increase the error. Therefore as suggested it is advisable to wait for the phasor to sweep over a certain angle and then take the measurements. In their method they have suggested an angle of 0.5 radians, on which case the time required for measurement comes out to be

$$T = \frac{0.5}{2\pi \Delta f} \quad (28)$$

Therefore it is evident that smaller frequency deviations will take larger time to measure and larger deviations smaller.

APPENDIX D

RECURSIVE UPDATE

Referring to Phadke Thorp's method a recursive update for SC DFT can be stated as,

$$V_{Ac}^{w+1}(m) = V_{Ac}^w(m) + \frac{2}{18N} \left[(v_w^A - v_{w-N}^A) \cos((w - (N+1)) \frac{2\pi m}{N}) \right] + \frac{2}{18N} \left[(v_w^B - v_{w-N}^B) \cos((w - \frac{2N}{3} - (N+1)) \frac{2\pi m}{N}) \right] + \frac{2}{18N} \left[(v_w^C - v_{w-N}^C) \cos((w - \frac{N}{3} - (N+1)) \frac{2\pi m}{N}) \right]$$

$$\begin{aligned}
V_{As}^{w+1}(m) &= V_{As}^w(m) \\
&+ \frac{2}{18N} \left[(v_w^A - v_{w-N}^A) \sin\left((w - (N+1)) \frac{2\pi m}{N}\right) \right] \\
&+ \frac{2}{18N} \left[(v_w^B - v_{w-N}^B) \sin\left((w - \frac{2N}{3} - (N+1)) \frac{2\pi m}{N}\right) \right] \\
&+ \frac{2}{18N} \left[(v_w^C - v_{w-N}^C) \sin\left((w - \frac{N}{3} - (N+1)) \frac{2\pi m}{N}\right) \right]
\end{aligned}$$

Similarly for B phase,

$$\begin{aligned}
V_{Bc}^{w+1}(m) &= V_{Bc}^w(m) \\
&+ \frac{2}{18N} \left[(v_w^B - v_{w-N}^B) \cos\left((w - (N+1)) \frac{2\pi m}{N}\right) \right] \\
&+ \frac{2}{18N} \left[(v_w^C - v_{w-N}^C) \cos\left((w - \frac{2N}{3} - (N+1)) \frac{2\pi m}{N}\right) \right] \\
&+ \frac{2}{18N} \left[(v_w^A - v_{w-N}^A) \cos\left((w - \frac{N}{3} - (N+1)) \frac{2\pi m}{N}\right) \right]
\end{aligned}$$

$$\begin{aligned}
V_{Bs}^{w+1}(m) &= V_{Bs}^w(m) \\
&+ \frac{2}{18N} \left[(v_w^B - v_{w-N}^B) \sin\left((w - (N+1)) \frac{2\pi m}{N}\right) \right] \\
&+ \frac{2}{18N} \left[(v_w^C - v_{w-N}^C) \sin\left((w - \frac{2N}{3} - (N+1)) \frac{2\pi m}{N}\right) \right] \\
&+ \frac{2}{18N} \left[(v_w^A - v_{w-N}^A) \sin\left((w - \frac{N}{3} - (N+1)) \frac{2\pi m}{N}\right) \right]
\end{aligned}$$

and for C phase,

$$\begin{aligned}
V_{Cc}^{w+1}(m) &= V_{Cc}^w(m) \\
&+ \frac{2}{18N} \left[(v_w^C - v_{w-N}^C) \cos\left((w - (N+1)) \frac{2\pi m}{N}\right) \right] \\
&+ \frac{2}{18N} \left[(v_w^A - v_{w-N}^A) \cos\left((w - \frac{2N}{3} - (N+1)) \frac{2\pi m}{N}\right) \right] \\
&+ \frac{2}{18N} \left[(v_w^B - v_{w-N}^B) \cos\left((w - \frac{N}{3} - (N+1)) \frac{2\pi m}{N}\right) \right]
\end{aligned}$$

$$\begin{aligned}
V_{Cs}^{w+1}(m) &= V_{Cs}^w(m) \\
&+ \frac{2}{18N} \left[(v_w^C - v_{w-N}^C) \sin\left((w - (N+1)) \frac{2\pi m}{N}\right) \right] \\
&+ \frac{2}{18N} \left[(v_w^A - v_{w-N}^A) \sin\left((w - \frac{2N}{3} - (N+1)) \frac{2\pi m}{N}\right) \right] \\
&+ \frac{2}{18N} \left[(v_w^B - v_{w-N}^B) \sin\left((w - \frac{N}{3} - (N+1)) \frac{2\pi m}{N}\right) \right]
\end{aligned}$$

REFERENCES

- [1] M. M. Begovic, P. M. Djurc, S. Dunlap, and A. G. Phadke, "Frequency tracking in power networks in the presence of harmonics," *IEEE Trans. Power Del.*, vol. 8, no.5, pp. 480–486, Apr. 1993.
- [2] C. T. Nguyen and K. Srinivasan, "A new technique for rapid tracking of frequency deviations based on level crossing," *IEEE Trans. Power Del.*, vol. PAS-103, no.8, pp. 2230–2236, Aug. 1984.
- [3] M. S. Sachdev and M. M. Giray, "A least error squares technique for determining power system frequency," *IEEE Trans. Power Del.*, vol. PAS-104, no.2, pp. 437–443, Feb. 1985.
- [4] A. A. Girgis and R. G. Brown, "Application of kalman filter in computer relaying," *IEEE Trans. Power App. Syst.*, vol. PAS-100, no.7, pp. 3387–3395, Jul. 1981.
- [5] A. A. Girgis and T. L. Hwang, "Optimal estimation of voltage phasors and frequency deviation using linear and non-linear kalman filtering: theory and limitations," *IEEE Trans. Power App. Syst.*, vol. PAS-103, no.10, pp. 2943–2951, Oct. 1984.
- [6] A. A. Girgis and F. H. Ham, "A new fft-based digital frequency relay for load-shedding," *IEEE Trans. Power App. Syst.*, vol. PAS-101, no.2, pp. 433–439, Feb. 1982.
- [7] J. Chen, "Accurate frequency estimation with phasor angles," Master's thesis, Bradley Dept. Elect. Comput. Eng. Virginia Polytechnic Inst. State Univ., Blacksburg, VA, 1994.
- [8] B. C. Lovell and R. C. W. B. Boashash, "The relationship between instantaneous frequency and time-frequency representations," *IEEE Trans. Signal Process.*, vol. 41, no.3, pp. 1458–1461, Mar. 1993.
- [9] D. Fan and V. Centeno, "Phasor-based synchronised frequency measurement in power systems," *IEEE Trans. Power Del.*, vol. 22, no.4, pp. 2010–2016, Oct. 2007.
- [10] A. G. Phadke and J. S. Thorp, *Computer Relaying for Power Systems*. New York: Research Studies Press, 1988.
- [11] V. Eckhardt, P. Hippe, and G. Hosemann, "Dynamic measuring of frequency and frequency oscillation in multi-phase power systems," *IEEE Trans. Power Del.*, vol. 4, no.1, pp. 95–102, Jan. 1989.
- [12] A. G. Phadke, J. S. Thorp, and M. G. Adamiak, "A new measurement technique for tracking voltage phasors, local frequency, and rate of change of frequency," *IEEE Trans. Power App. Syst.*, vol. PAS-102, no.5, pp. 1025–1038, May 1983.

Sanjay Dambhare is currently working towards Ph.D. degree in Department of Electrical Engineering at Indian Institute of Technology, Bombay, India. His research interests include power system protection, large scale power system analysis.

Rajeev Kumar Gajbhiye is currently working towards Ph.D. degree in Department of Electrical Engineering at Indian Institute of Technology, Bombay, India. His research interests include large scale power system analysis, power system protection and deregulation.

Chetan J. Tonde is undergraduate student in the Department of Electrical Engineering at College of Engineering Pune, India. His research interest lies mainly in statistical signal processing and their applications for power systems.

Sandesh A. Gandhi is undergraduate student in the Department of Electrical Engineering at College of Engineering Pune, India. His research interests include digital signal processing and its applications in power electronics.

S. A. Soman is Professor in the Department of Electrical Engineering at Indian Institute of Technology Bombay, India. He has authored a book on Computational Methods for Large Sparse Power System Analysis: An Object Oriented Approach, published by Kluwer Academic Publishers in 2001. His research interests include power system analysis, power system protection and optimization.

Mukul C. Chandorkar is Professor in the Department of Electrical Engineering at Indian Institute of Technology Bombay, India.